

EKF-based Carrier Tracking in One-bit Quantized GNSS Receiver

Ao Peng, Gang Ou* and Jianghong Shi

*School of Information Science and Engineering, Xiamen University, China
pa@xmu.edu.cn, ougang@xmu.edu.cn, shijh@xmu.edu.cn*

Abstract

Coarse resolution quantizers are widely used in commercial GNSS receivers to reduce the cost and power consumption. However, when the coarse resolution quantizers are used nonlinear distortion is introduced to the received signals and should be taken into consideration. In this paper, a carrier tracking algorithm based on extended kalman filter (EKF) is proposed for 1-bit quantized GNSS signals. The observation model for 1-bit quantized signals is established theoretically. An approximation of the observation function is proposed and analyzed numerically. Performance of the proposed algorithm is evaluated by simulation, compared with both PLL using 1-bit phase discriminator and EKF using high-resolution samples.

Keywords: *Carrier Tracking, GNSS Receiver, Extended Kalman Filters, One-bit Quantization*

1. Introduction

Due to the advantages of simplicity and low power consumption, low cost analog-to-digital converters (ADCs) with small quantization length, especially the 1-bit ADCs are widely used in commercial GNSS receivers. However, most of the current baseband processing techniques assume the received signals have arbitrary high precision. When a 1-bit ADC is used, the signal distortion introduced by nonlinear quantization operation should be taken into consideration. The 1-bit ADC quantization loss is up to 1.96dB [1]. In this paper, carrier tracking in 1-bit quantized GNSS receivers is discussed.

Various kinds of methods were proposed to reduce the performance degradation caused by 1-bit quantization. The effective noise model of 1-bit quantization and its effect on the time-delay estimation in a GNSS receiver was discussed in [2]. Adjustments in the front-end of a digital GNSS receiver were suggested in [3, 4]. By redesigning the front-end filter and quantizer, or by increasing the sampling frequency, the effective signal-to-noise ratio (SNR) after quantization can be improved.

In carrier tracking, the accuracy of phase estimation degrades greatly because of 1-bit quantization when the traditional arctangent phase discriminator is used. To reduce the estimation error, some new discriminators have been proposed based on the property of the quantized signal [5-9]. A digital phase discriminator (DPD) using the 1-bit quantized signal was first proposed in [5]. The accuracy of the discriminator can be improved by increasing the sampling rate. Then the updated versions of the digital phase discriminator were proposed, including a noise balanced digital phase discriminator (NB-DPD) [6], a robust digital phase discriminator (RDPD) [8], and a SNR aided accuracy phase discriminator (SAPD) [9].

In the typical applications of GNSS receiver, the carrier phase, as well as the carrier frequency, is changing continuously due to the relative motion of the satellite and receiver. The most commonly used technologies in carrier tracking include Phase Lock Loop (PLL) and kalman filter. When used in carrier tracking, a kalman filter implementation is equivalent

to a PLL with adaptive noise bandwidth [10]. However, the kalman filter is originally designed for linear system. Various alterations of kalman filter have been designed for parameter tracking of 1-bit quantized signals. A kalman filter using the sign of innovations [11] was proposed to limit the quantization length requirement in wireless sensor networks. A kalman like particle filter [12] and an unscented kalman filter [13] were also proposed to solve different kinds of parameter tracking problems with quantized measurements. The convergence of kalman filter using quantized measurements was analyzed in [14]. The applications listed above indicate that the Kalman filtering technology is effective when used in parameter estimation of quantized signals.

In this paper, an extended kalman filter (EKF) based carrier tracking algorithm is proposed for 1-bit quantized GNSS receiver. Chapter 2 describes the signal model and its relative property. In chapter 3, an EKF based carrier tracking algorithm is proposed. The approximation of the observation function is given in chapter 4, and chapter 5 shows the simulation results.

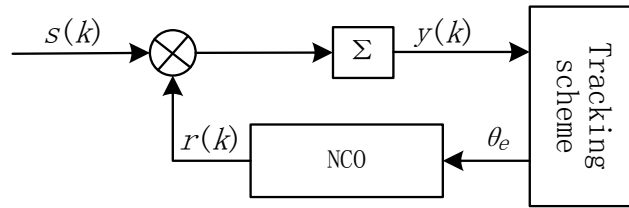


Figure 1. Typical Carrier Tracking Scheme in GNSS Receivers

2. Problem Description

A typical carrier tracking scheme in a GNSS receiver with 1-bit ADC is shown in Figure 1. The received signal after quantization is given by

$$s(k) = \text{sgn} \left[\sqrt{2P} \cos(\omega_c k T_s + \theta_0 + 0.5 \omega_a k^2 T_s^2) + n(k) \right] \quad (1)$$

where P is the receiving power of GNSS signal, ω_c is the intermediate frequency including Doppler shift, T_s is the sampling interval, θ_0 is the initial carrier of the received signal, ω_a is the Doppler rate caused by the acceleration of relative motion between and satellite and receiver. The higher order dynamics of the relative motion is ignored. $n(k)$ is the additive white Gaussian noise (AWGN) with power σ^2 , and $\text{sgn}(x)$ denotes the polarity function of x .

The local carrier replica is a periodic square wave with I/Q branches which is given by

$$r(k) = \text{sgn}[\cos(\omega_o k T)] + j \text{sgn}[\sin(\omega_o k T_s)] \quad (2)$$

where ω_o is the output frequency of the numerical control oscillator (NCO). The signal after mixing and accumulating is given by

$$y = \frac{1}{N} \sum_{k=0}^{N-1} s(k)r(k) \quad (3)$$

where N is the number of samples during the accumulation period T . In most commercial applications, ω_c , ω_o , ω_a and NT_s meet the following condition when the receiver keeps continuous tracking of the carrier

$$\frac{\omega_o - \omega_c + \omega_a NT_s}{\omega_c} \approx 0 \quad (4)$$

Then we have

$$y \approx \frac{1}{N} \sum_{k=0}^{N-1} \text{sgn} \left[\sqrt{2P} \cos(\phi_k + \theta_e) + n_i \right] + j \frac{1}{N} \sum_{k=0}^{N-1} \text{sgn} \left[\sqrt{2P} \sin(\phi_k + \theta_e) + n_q \right] \quad (5)$$

where $\phi_k = \omega_c k T_s$ and θ_e is the average phase error during the accumulation period, which is given by [15]

$$\theta_e = \theta_0 + \frac{N}{2} (\omega_c - \omega_o) T_s + \frac{N^2}{6} \omega_a T_s^2 \quad (6)$$

DPD [5] uses the ratio of negative samples of $y(k)$ to estimate the phase error. The ratio is given by

$$\eta_i = \frac{N - y_I}{2N}, \eta_q = \frac{N - y_Q}{2N} \quad (7)$$

where y_I and y_Q are the real part and imaginary part of y , respectively. The DPD is defined by

$$\theta_e = \text{sgn}(\eta_q - 0.5) \eta_i \pi \quad (8)$$

For high-SNR applications, the NB-DPD was proposed to reduce estimation deviation, which is given by [6]

$$\theta_e = \text{sgn}(y_Q) \frac{\pi}{2} \left(1 - \frac{y_I}{|y_I| + |y_Q|} \right) \quad (9)$$

For moderate-SNR applications, the SAPD was proposed to compensate the noise effect [9], which is given by

$$\theta_e = \arg \min \left\{ [y_I - E(y_I)]^2 + [y_Q - E(y_Q)]^2 \right\} \quad (10)$$

where $E(x)$ is the mean value of variable x . Equation (10) can be solved by Newton's method. The relationship between noise and estimation error was analyzed in [8], and the RDPD using iterative method was proposed to achieve higher accuracy and better noise robustness.

In the next chapter, an extended kalman filter based tracking algorithm is proposed. Instead of using the phase discriminators listed above, the measurement model of the EKF is directly derived from the output of accumulator.

3. EKF-Based Tracking Algorithm

According to(1), the estimated parameters include phase difference, frequency difference and Doppler rate. The system model is given by [15]

$$X_{k+1} = AX_k + W_n = \begin{bmatrix} 1 & NT_s & N^2T_s^2/2 \\ 0 & 1 & NT_s \\ 0 & 0 & 1 \end{bmatrix} \begin{bmatrix} \theta_0 \\ \omega_c - \omega_o \\ \omega_a \end{bmatrix}_k + W_n \quad (11)$$

where $X = [\theta_0 \ \omega_c - \omega_o \ \omega_a]^T$ is the state vector, A is the system dynamic matrix and W_n is the system noise mainly determined by the quality of receiver clock [16]. The spectral intensity matrix Q of W_n is given in [17].

Only the imaginary part of $y(k)$ is used to establish the measurement model of the EKF. The mean value of y_Q is given by

$$E[y_Q] = \frac{1}{N} \sum_{k=0}^{N-1} \left\{ 1 - \operatorname{erfc} \left[\sqrt{\frac{2P}{\sigma^2}} \cos(\phi_k + \theta_e) \right] \right\} \operatorname{sgn}(\sin \phi_k) \quad (12)$$

Notice the mean value of y_Q is a function of phase error θ_e and $SNR = P/\sigma^2$. Let $\lambda = \sqrt{2SNR}$ and $h(\theta_e, \lambda) = E[y_Q]$. The relationship between y_Q and $h(\theta_e, \lambda)$ is given by

$$y_Q = h(\theta_e, \lambda) + v \quad (13)$$

where v is residual error defined by

$$v = \frac{1}{N} \sum_{k=0}^{N-1} \left\{ s(k) - 1 + \operatorname{erfc} \left[\lambda \cos(\phi_k + \theta_e) \right] \right\} \operatorname{sgn}(\sin \phi_k) \quad (14)$$

where $\operatorname{erfc}(x)$ is the complementary error function defined by

$$\operatorname{erfc}(x) = \frac{2}{\sqrt{\pi}} \int_x^{\infty} \exp(-t^2) dt \quad (15)$$

Lemma: v is white noise with zero mean when N is sufficiently large.

Proof: it has been proved that ϕ_k is uniformly distributed in a circle when N is sufficiently large [5]. So the summation in (14) can be replaced by definite integral on the circle as follows

$$v = \frac{1}{2\pi} \int_{-\pi}^{\pi} \left[\operatorname{sgn}(\sqrt{2P} \cos \phi + n) - 1 + \operatorname{erfc}(\lambda \cos \phi) \right] \operatorname{sgn}[\sin(\phi - \theta_e)] d\phi \quad (16)$$

where n is the AWGN term in (1). It's obvious from (16) that $v(k)$ is time-independent. For different time slot i and j , we have $E[v_i v_j] = E[v_i] E[v_j]$. The mean value of v is

$$\begin{aligned} E[v] &= \frac{1}{2\pi} \int_{-\pi}^{\pi} \frac{1}{2} \operatorname{erfc}(\lambda \cos \phi) [-2 + \operatorname{erfc}(\lambda \cos \phi)] r(\phi - \theta_e) d\phi \\ &+ \frac{1}{2\pi} \int_{-\pi}^{\pi} \left[1 - \frac{1}{2} \operatorname{erfc}(\lambda \cos \phi) \right] \operatorname{erfc}(\lambda \cos \phi) r(\phi - \theta_e) d\phi = 0 \end{aligned} \quad (17)$$

and we have

$$E[v(i)v(j)] = R_v \delta(i - j) \quad (18)$$

where $\delta(x)$ is the Dirac delta function and R_v is the variance of v .

$$\begin{aligned} R_v &= \frac{1}{2\pi} \int_{-\pi}^{\pi} \frac{1}{2} \operatorname{erfc}(\lambda \cos \phi) [-2 + \operatorname{erfc}(\lambda \cos \phi)]^2 d\phi \\ &+ \frac{1}{2\pi} \int_{-\pi}^{\pi} \left[1 - \frac{1}{2} \operatorname{erfc}(\lambda \cos \phi) \right] \operatorname{erfc}^2(\lambda \cos \phi) d\phi \\ &= \frac{1}{2\pi} \int_{-\pi}^{\pi} [2 - \operatorname{erfc}(\lambda \cos \phi)] \operatorname{erfc}(\lambda \cos \phi) d\phi \end{aligned} \quad (19)$$

Equation (13) is used as the measurement model with observation y_Q and the observation noise v .

The prediction and update process is given as follows

$$X_{k+1|k} = AX_k, P_{k+1|k} = AP_k A^T + Q \quad (20)$$

$$X_{k+1} = X_{k+1|k} + L_k [y_{Qk} - h(\eta X_{k+1|k}, \lambda_k)], P_{k+1} = (I - L_k H_k) P_{k+1|k} \quad (21)$$

where P_k is the estimate covariance at time slot k , $\eta = [1 \quad NT_s/2 \quad N^2 T_s^2/6]$ and H_k is the observing matrix derived by

$$H_k = \frac{\partial h(\theta_e, \lambda_k)}{\partial X} \quad (22)$$

The optimal Kalman gain L_k is given by

$$L_k = P_{k+1|k} H_k^T (H P_{k+1|k} H^T + R_v)^{-1} \quad (23)$$

4. Approximation of Observation Function

Rewrite the observation function in definite integral form and we get

$$h(\theta_e, \lambda) = \frac{1}{2\pi} \int_{-\pi}^{\pi} \{ [1 - \operatorname{erfc}(\lambda \cos \phi)] \operatorname{sgn}[\sin(\phi - \theta_e)] \} d\phi \quad (24)$$

Equation (24) can also be represented as a power series [9]. However, both of them are inconvenient to be used in real time applications due to their computational complexities. In this chapter, an approximation of the observation function with high accuracy and slight computational complexity is proposed.

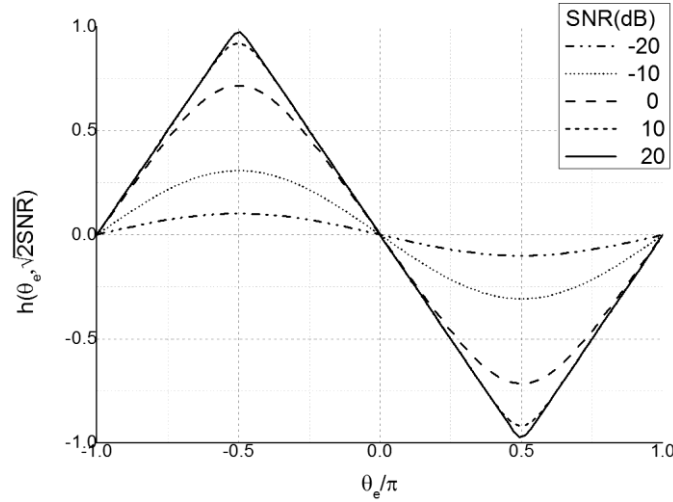


Figure 2. The Observation Function for Different SNR

Figure 2 shows curves of the observation function versus θ_e/π for different values of SNR. For a certain SNR, the maximum value of $h(\theta_e, \lambda)$ is obtained as $\theta_e = -\frac{1}{2}\pi$. And it's obvious when $\theta_e \in \left[-\frac{1}{2}\pi, \frac{1}{2}\pi\right]$, $h(\theta_e, \lambda)$ is monotone to θ_e . The maximum value of $h(\theta_e, \lambda)$ is given by

$$h_\lambda(\lambda) = h\left(-\frac{\pi}{2}, \lambda\right) = 1 - \frac{1}{2\pi} \int_{-\pi}^{\pi} \operatorname{erfc}(\lambda \cos \phi) d\phi \quad (25)$$

which defines the amplitude function of $h(\theta_e, \lambda)$. When the SNR is high, the observation function changes linearly versus θ_e in the monotone area, such as the curves in Figure 2 when SNR=10dB and SNR=20dB. For low SNR, the observation function is similar to a negative sine function, e.g. the curves when SNR is no more than 0dB. The linear approximation is given by

$$h_t(\theta_e, \lambda) = \frac{-2h_\lambda(\lambda)}{\pi} \theta_e \quad (26)$$

and the trigonometric approximation is given by

$$h_s(\theta_e, \lambda) = -h_\lambda(\lambda) \sin(\theta_e) \quad (27)$$

The relative power error, also called distortion ratio, is used to evaluate the accuracy of the two approximations, which is defined by

$$\varepsilon_{l,s}(\lambda) = \frac{\int_{-\pi/2}^{\pi/2} [h_{l,s}(\theta_e, \lambda) - h(\theta_e, \lambda)]^2 d\theta_e}{\int_{-\pi/2}^{\pi/2} h^2(\theta_e, \lambda) d\theta_e} \quad (28)$$

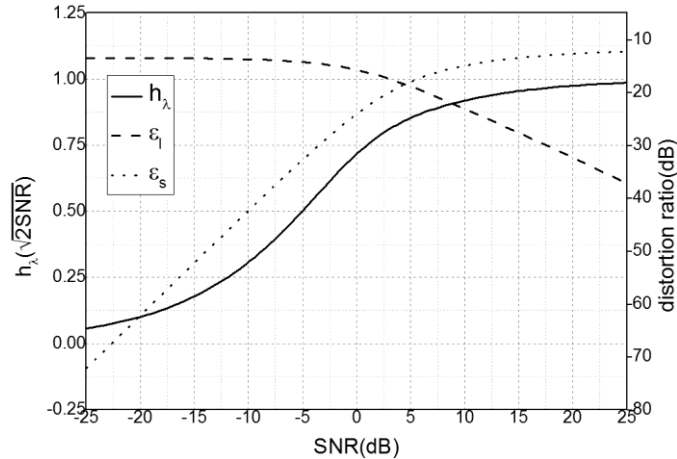


Figure 3. The Amplitude Function and the Distortion Ratio vs. SNR

In Figure 3, the dash line shows the distortion ratio of the linear approximation ε_l , and the dot line shows the distortion ratio of the trigonometric approximation ε_s . Both of the distortion ratios are measured in decibel. ε_l decreases as the SNR rises, while ε_s increases. Both of the two distortion ratios are lower than -10dB, which means the two approximations are accurate. When $SNR \approx 4.7dB$, $\varepsilon_l = \varepsilon_s \approx -19dB$. So a better way is to use different approximation models due to SNR. When the SNR is higher than 4.7dB, the linear approximation is chosen, and when the SNR drops below 4.7dB, the trigonometric approximation is chosen. The overall distortion ratio is no more than -19dB and can be neglected. Figure 3 also shows the amplitude function in solid line. The amplitude function is time-invariant, and its value is only depended on the SNR. In real time applications, the value of amplitude function can be pre-calculated and stored in a lookup table to replace runtime computation.

5. Simulations

The performance of the proposed carrier tracking algorithm is tested by simulation. The results are compared with a traditional phase lock loop (PLL) using NB-DPD and an EKF using analog signals (with arbitrary high precision). The parameters of the simulated signal are set as follows. The sampling frequency is 16.384MHz, the intermediate frequency is 4.092MHz, and the Doppler rate is 51.5Hz/s (the relevant acceleration is $9.8m/s^2$). The accumulation period $T = 1ms$. The system noise variance Q is calculated using the typical Allan variance parameters for crystal clocks [17]. In addition, a second-order PLL is used for comparison. The bandwidth of the PLL is 10Hz, and the damping coefficient of the PLL is 0.707.

Figure 4 shows the phase tracking error obtained under two different scenarios. The SNRs in the upper two subfigures are -20dB, and the SNRs in the lower subfigures are 10dB. The two scenarios cover two approximation models described in Section IV. The simulation time is 1 second. The phase error decreases if EKF is used. And for PLL, the phase error fluctuates with a constant maximum amplitude. The steady-state error of EKF is also significantly smaller than the PLL. The main reason is the equivalent noise bandwidth of the EKF in steady state is much smaller than PLL. When used in the PLL, the advantage of well-designed 1-bit phase discriminators such as DPD or NB-DPD is negligible.

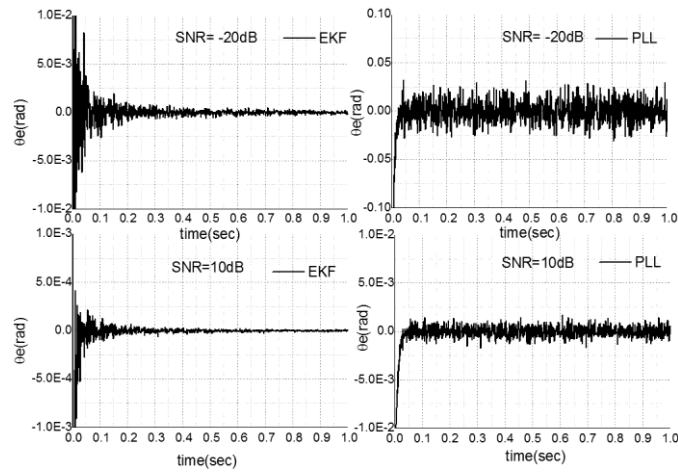


Figure 4. Tracking Error of Carrier

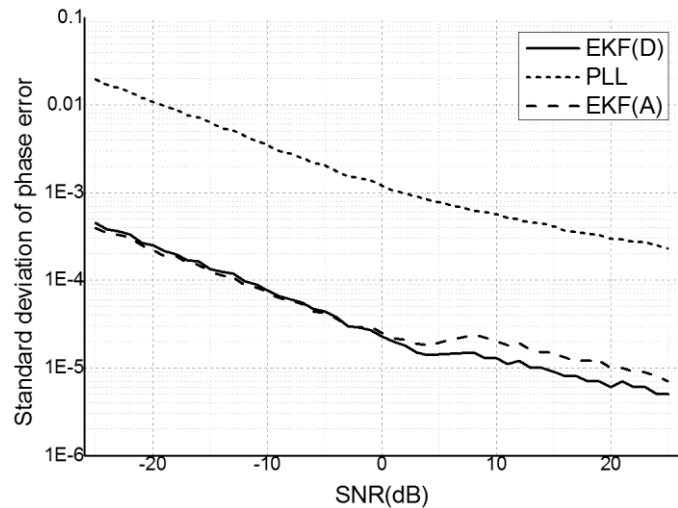


Figure 5. Standard Deviation of Steady-state Error vs. SNR

Figure 5 shows the relationship between standard deviation of phase error and SNR. The legend EKF (D) stands for the proposed EKF using 1-bit quantized signals, and the legend EKF (A) stands for the compared EKF using high-resolution samples. The curves are obtained through Monte Carlo simulations, which illustrate the levels of steady-state tracking error. The difference of the standard deviations by using EKF or PLL is significant. When the SNR is -20dB, the standard deviation of phase error using PLL is about 0.01 radius, and the standard deviation using the proposed EKF is about $2e-4$ radius. The latter is almost 48 times smaller than the former. The phase error in steady-state reduces as SNR become higher. No matter how the SNR changes, the EKF based tracking algorithm always keeps an obvious superiority to PLL. When the SNR is 20dB, the standard deviation using the proposed EKF is still about 44 times smaller than that of using the PLL.

The performance of quantization loss reduction can be concluded by comparing the steady-state phase error of EKF (D) and EKF (A). When SNR is lower than 4.7dB, the trigonometric approximation of the observation function is used in EKF (D), and the

steady-state tracking error is very close to EKF (A). The SNR loss introduced by 1-bit quantization is overcome. What's more, when the SNR is higher than 4.7dB, the linear approximation is used, and the standard deviation using EKF (D) is even smaller than EKF(A). It's because in such a case, the observation model is linear, and EKF (D) becomes a standard kalman filter. While EKF (A) uses a nonlinear observation model, and the linearization of the observation model introduces additional SNR loss.

6. Conclusions

In this paper, an extended kalman filtering base carrier tracking algorithm for GNSS receivers using one-bit quantizers is proposed. The mathematics model of the observation is established and analyzed. The derived observation function is given in integral expression. To simplify the calculation, an approximation of the observation function with low computational complexity is given. The accuracy of the approximation is evaluated by distortion ratio, which is calculated by relative power error method. The performances of the proposed approach is tested by Monte Carlo simulations, compared with PLL using 1-bit phase discriminators and EKF using high-resolution samples. Simulation results shows that the steady-state tracking error is significantly reduced in comparison with the PLL, and the quantization loss is also eliminated by comparing with the EKF using high-resolution samples.

Acknowledgements

This work was supported by Xiamen Satellite Navigation R&D Test Base, funding number 3502Z20121010.

References

- [1] H. Chang, "Presampling filtering, sampling and quantization effects on the digital matched filter performance", in ITC/USA'82; Proceedings of the International Telemetry Conference, (1982), pp. 889-915.
- [2] F. Wendler, M. Stein, A. Mezghani, and J. A. Nossek, "Quantization-loss reduction for 1-bit BOC positioning," in Proceedings of the ION International Technical Meeting (2013).
- [3] J. T. Curran, D. Borio, G. Lachapelle, and C. C. Murphy, "Reducing front-end bandwidth may improve digital GNSS receiver performance," Signal Processing, IEEE Transactions on, vol. 58, pp. 2399-2404 (2010)
- [4] M. Stein, F. Wendler, A. Mezghani, and J. A. Nossek, "Quantization-loss reduction for signal parameter estimation," in Acoustics, Speech and Signal Processing (ICASSP) 2013 IEEE International Conference on (2013)
- [5] C. F. Chang and M. S. Kao, "High accuracy carrier phase discriminator in one-bit quantized software-defined receivers," Signal Processing Letters, IEEE, vol. 15, (2008), pp. 397-400.
- [6] C. F. Chang, R. M. Yang, and M. S. Kao, "1-bit high accuracy carrier phase discriminators", Aerospace and Electronic Systems, IEEE Transactions on, vol. 49, (2013), pp. 160-174.
- [7] L. Xiaohui and H. Long, "Performance analysis of finite word-length effect on phase discriminator in satellite navigation receiver", Journal of national university of defense technology, vol. 35, (2013), pp. 89-92.
- [8] J. Zhao, J. Zhang, and J. Yin, "A robust digital phase discriminator in one-bit quantized software-defined receivers", in Wireless Communications, Networking and Mobile Computing, 2009, WiCom'09, 5th International Conference, (2009), pp. 1-4.
- [9] W. H. Hsieh, C. F. Chang, and M. S. Kao, "SNR-aided accurate phase estimation in 1-bit software-defined receiver", Aerospace and Electronic Systems, IEEE Transactions on, vol. 48, (2012), pp. 1570-1582.
- [10] C. R. Hamm, W. Flenniken, D. M. Bevely, and D. Lawrence, "Comparative performance analysis of aided carrier tracking loop algorithms in high noise/high dynamic environments", in Proceedings of the 2004 IONGNSS Conference (2004).
- [11] A. Ribero, G. B. Giannakis, and S. I. Roumeliotis, "SOI-KF: Distributed Kalman filtering with low-cost communications using the sign of innovations", Signal Processing, IEEE Transactions on, vol. 54, (2006), pp. 4782-4795.

- [12] R. T. Sukhavasi, and B. Hassibi, "The kalman like particle filter: optimal estimation with quantized innovations/measurements", in Decision and Control, 2009 held jointly with the 2009 28th Chinese Control Conference. CDC/CCC 2009. Proceedings of the 48th IEEE Conference on, **(2009)**.
- [13] Y. Zhou, J. Li, and D. Wang, "Unscented Kalman Filtering based quantized innovation fusion for target tracking in WSN with feedback", in Machine Learning and Cybernetics, 2009 International Conference on, **(2009)**.
- [14] K. You, L. Xie, S. Sun, and W. Xiao, "Quantized filtering of linear stochastic systems", Transactions of the Institute of Measurement and Control, vol. 33, **(2011)**, pp. 683-698.
- [15] M. L. Psiaki and H. Jung, "Extended Kalman filter methods for tracking weak GPS signals", in Proceedings of the 15th international Technical Meeting of the Satellite Division of The Institute of Navigation (ION GPS 2002), **(2002)**.
- [16] R. G. Brown and P. Y. Hwang, "Introduction to random signals and applied Kalman filtering", vol. 1, John Wiley & Sons, New York, **(1992)**.
- [17] N. Ziedan and J. Garrison, "Bit synchronization and Doppler frequency removal at very low carrier to noise ratio using a combination of the Viterbi algorithm with an extended kalman filter", in Proceedings of the 16th International Technical Meetins of the Satellite Division of the Intitute of Navigation (ION GPS/GNSS 2003), **(2003)**.